Review

Cardiac Magnetic Resonance Imaging for the Investigation of Cardiovascular Disorders.

Part 1: Current Applications

Ajit H. Goenka, MD
Scott D. Flamm, MD, MBA

Cardiac magnetic resonance imaging is a robust noninvasive technique for investigating cardiovascular disorders. The evolution of cardiac magnetic resonance and its widening span of diagnostic and prognostic applications have generated excitement as well as uncertainty regarding its potential clinical use and its role vis-à-vis conventional imaging techniques. The purpose of this evidence-based review is to discuss some of these issues by highlighting the current (Part 1) and emerging (Part 2) applications of cardiac magnetic resonance. Familiarity with the versatility and usefulness of cardiac magnetic resonance will facilitate its wider clinical acceptance for improving the management of cardiovascular disorders. ***(Tex Heart Inst J 2014;41(1):7-20)***

Key words: *Cardiomyopathies/diagnosis; fibrosis; gadolinium DTPA/diagnostic use; hypertrophy, left ventricular/diagnosis; magnetic resonance angiography; magnetic resonance imaging/standards; myocarditis/diagnosis; pericarditis, constrictive/diagnosis; sarcoidosis; stroke volume; ventricular dysfunction, left/diagnosis*

From: *Cardiovascular Imaging Laboratory, Imaging Institute; and Cardiovascular Medicine, Heart and Vascular Institute; Cleveland Clinic, Cleveland, Ohio 44195*

Address for reprints: *Scott D. Flamm, MD, MBA, Cardiovascular Imaging Laboratory, J1-4, Imaging Institute, Cleveland Clinic, 9500 Euclid Ave., Cleveland, OH 44195*

E-mail: *flamms@ccf.org*

Cardiac magnetic resonance imaging (CMR) has emerged as a robust noninvasive technique for the investigation of cardiovascular disorders. Several technical advances have facilitated the growth of CMR by enabling high-quality diagnostic imaging despite the challenges inherent to cardiac imaging: cardiorespiratory motion and flowing blood. Considerable research evidence and years of clinical experience have shown the diagnostic and prognostic usefulness of CMR in a wide spectrum of cardiovascular disorders. The coming-of-age of CMR and its widening span of applications have generated excitement, as well as uncertainty, regarding its potential clinical use and its role vis-à-vis conventional imaging techniques. The purpose of this article is to highlight the current (Part 1) and emerging (Part 2) applications of CMR, in order to assist the referring physician in the decision-making process.

Current Applications

Analysis of Ventricular Function and Volumes

Cardiac magnetic resonance imaging has evolved into an accurate and well-validated tool for the evaluation of cardiac function. The high reproducibility of CMR-derived measures of cardiac function makes CMR an ideal technique for the longitudinal follow-up of patients.[1] This superior reproducibility has also led to increased use of CMR as a reference standard for other techniques and as a surrogate outcome measure in drug studies. In fact, the use of CMR has facilitated reduction in the required sample sizes for such studies by as much as 10-fold, in turn decreasing overall study costs by up to 80%.[2-4]

Cardiac-function evaluation on CMR is based on true volumetric quantification, which is performed by dividing the ventricles into several smaller and relatively simpler subvolumes for the calculation of global ventricular volume (the disc-summation technique). This technique does not use the geometric assumptions that form the basis of planar imaging techniques like echocardiography. The current workhorse of functional CMR is the balanced steady-state free precession (SSFP) sequence, which provides excellent delineation of the endocardial–blood pool interface. When combined with parallel imaging techniques, the SSFP sequence enables the acquisition of electrocardiographic (ECG)-gated images within breath-hold times as short as 6 seconds per slice while maintaining sufficient spatial resolution. Images are acquired in the true short-axis plane from the base of the heart to the apex (Fig. 1). For image

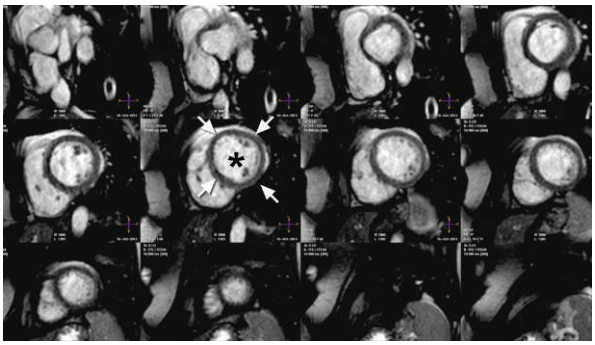

Fig. 1 *Panel of cine steady-state free precession images along the short axis of the left ventricle (LV). The asterisk denotes the LV cavity blood pool and the white arrows point to the epicardial surface. Cardiac function is calculated by manual contouring of the endocardial and epicardial surfaces from the base to the apex of the LV. Note the high contrast between the endocardial blood-pool interfaces.*

analysis, representative end-diastolic (ED) and end-systolic (ES) frames are chosen from the acquired dataset. For the calculation of right ventricular (RV) volumes, a transverse plane is often preferred over the short-axis view, because the interface between the RV and the right atrium on the basal slices is better delineated on the transverse plane.

The cine magnetic resonance (MR) dataset acquired via the SSFP sequence is also used to evaluate regional segmental contributions and, through visual estimation of wall motion on a movie of the beating heart, the synchronization of physiologic mechanical events between myocardial segments. Quantitative analysis of absolute or percentage regional systolic wall-thickening can also be performed. Another MR technique, myocardial tagging, collects information about the shape and dimensions of the ventricle at different time points throughout the cardiac cycle by noninvasively creating a grid of lines that track the underlying myocardial deformation. This technique is used for complex analyses of strain and regional ventricular morphology (wall thickness and radii of curvature).

Magnetic resonance imaging is also emerging as a valuable technique complementary to Doppler echocardiography for the analysis of diastolic function. Elevated left ventricular (LV) filling pressure and chronic diastolic dysfunction are important causes of left atrial dilation. On CMR, left atrial planimetry is performed on an SSFP 4-chamber view. An area of 24 cm^2 is considered the upper limit of normal left atrium.[5] Ventricular filling curves can be obtained from CMR, and various markers of diastolic function (peak filling rate, time to peak filling rate, and peak of late filling) can be calculated from these curves. Phase-contrast MR imaging (PC-MR) , a versatile technique that primarily measures velocities and flow, can also be used to evaluate diastolic function. With PC-MR, transtricuspid or transmitral velocities can be mapped and then used for the calculation of time-velocity curves, a technique analogous to the method used in Doppler echocardiography. In addition, PC-MR can be used to analyze flow patterns in the pulmonary and caval veins, in turn providing indirect information about the diastolic function of the respective ventricles. Increased LV stiffness due to myocardial fibrosis is another important mechanism of diastolic dysfunction. Myocardial fibrosis can be noninvasively characterized with delayed-enhancement MR imaging (DE-MR) and quantitative T1 mapping (see below and Part 2). Other research tools for the evaluation of diastolic function include PC-MR evaluation of myocardial tissue velocities, MR spectroscopy, and MR elastography.

Analysis of Myocardial Viability

Cardiac magnetic resonance imaging is so reliable as a noninvasive method for identifying scarred myocardium in patients with myocardial infarction (MI) that it has become the reference standard for this purpose. In the setting of myocardial dysfunction, the absence of scar suggests viability: the potential to improve or recover contractile function after revascularization. Therefore, this application of CMR is also called viability imaging. The current workhorse for viability evaluation is DE-MR, which is typically performed by means of a segmented gradient-recalled echo (GRE) sequence, after the administration of the MR contrast agent gadolinium. This technique also includes the application of an inversion-recovery (IR) preparatory pulse to nullify the signal from the normal myocardium.

Viability imaging has its basis in the principle that the concentration of gadolinium in infarcted myocardium is higher than that in normal myocardium several minutes after the administration of the contrast agent. Normal myocardium is composed of tightly packed muscle fibers with trivial extracellular space. However, in acutely infarcted myocardium, disruption of cell membranes results in rapid distribution of gadolinium into both the intracellular and interstitial spaces, which contributes to the increased distribution volume and retention of gadolinium. Similarly, chronically scarred myocardium has a higher interstitial component than normal myocardium. The consequent difference in concentration of gadolinium results in greater shortening of the T1 relaxation time. This manifests itself as relative hyperintensity, in comparison with surrounding normal myocardium on T1-weighted (T1W) images, and is referred to as late gadolinium enhancement (LGE). Irreversibly damaged tissue has a slower wash-in and wash-out of gadolinium: images are acquired 10 to 30 minutes after a bolus of gadolinium, in order that the difference in gadolinium concentration between normal and scarred myocardium will be clear. This practice, in combination with the IR preparatory

pulse that suppresses the normal myocardial signal, results in high contrast differential between the viable and scarred myocardium.

In segments with infarcted myocardium, LGE is typically subendocardial or transmural in location and follows a coronary artery distribution. However, segments with stunned or hibernating myocardium that have intact cell membranes do not exhibit LGE. Further, it should be emphasized that LGE of the infarcted myocardium requires intact microvessels. Large MIs might have central areas with disrupted capillaries and endarterioles, in such a manner that gadolinium is unable to reach the core of the reperfused infarcted area. These areas are denoted as microvascular obstruction and are seen as nonenhancing myocardium within the enhancing necrotic myocardial core.[6] Delayed-enhancement MR is also useful in the detection of thrombi associated with MI. Acute thrombi typically appear as nonenhancing intraventricular mass-like lesions (Fig. 2), whereas thrombi in a chronic setting are more typically seen as conforming to the contour of the ventricular cavity.

Delayed-enhancement MR directly reveals both the viable and nonviable myocardium with high spatial resolution. This enables the gradation of myocardial viability as a continuum in accordance with the transmural extent of LGE. There exists an inverse relationship between the extent of LGE and the likelihood of functional recovery after revascularization. Segments with <25% LGE relative to wall thickness are scored as viable, whereas those with >75% LGE are not expected to recover contractile function and are therefore scored as nonviable. Intermediate likelihood of recovery is expected in segments with 25% to 75% LGE.[7-9] Because of its high spatial resolution, DE-MR can also detect subendocardial infarcts that are missed by single-photon-emission computed tomography (SPECT).[10] Both animal and human studies have validated the robust clinical usefulness of DE-MR.[8,11]

It should be noted that DE-MR has limited use in the setting of diffuse myocardial fibrosis, which is beyond the spatial resolution of the current technique. This limitation accounts for the discrepancies that are sometimes observed between DE-MR and histologic findings.[12] Also, in patients with severe renal insufficiency (glomerular filtration rate, <30 mL/min/1.73 m^2), the use of gadolinium is contraindicated because of the risk of nephrogenic systemic fibrosis.[13]

Evaluation of Myocardial Perfusion and Ischemia

Myocardial perfusion imaging (MPI) using dynamic contrast-enhanced MR imaging (DCE-MR) has come to play an important role in the diagnosis of ischemic heart disease. Dynamic contrast-enhanced MR is a technically challenging application, given the competing demands of adequate anatomic coverage and high spatial and temporal resolution. Dynamic contrast-enhanced MR involves the acquisition of a series of T1W images during the first pass of intravenously administered gadolinium. The sequences available for DCE-

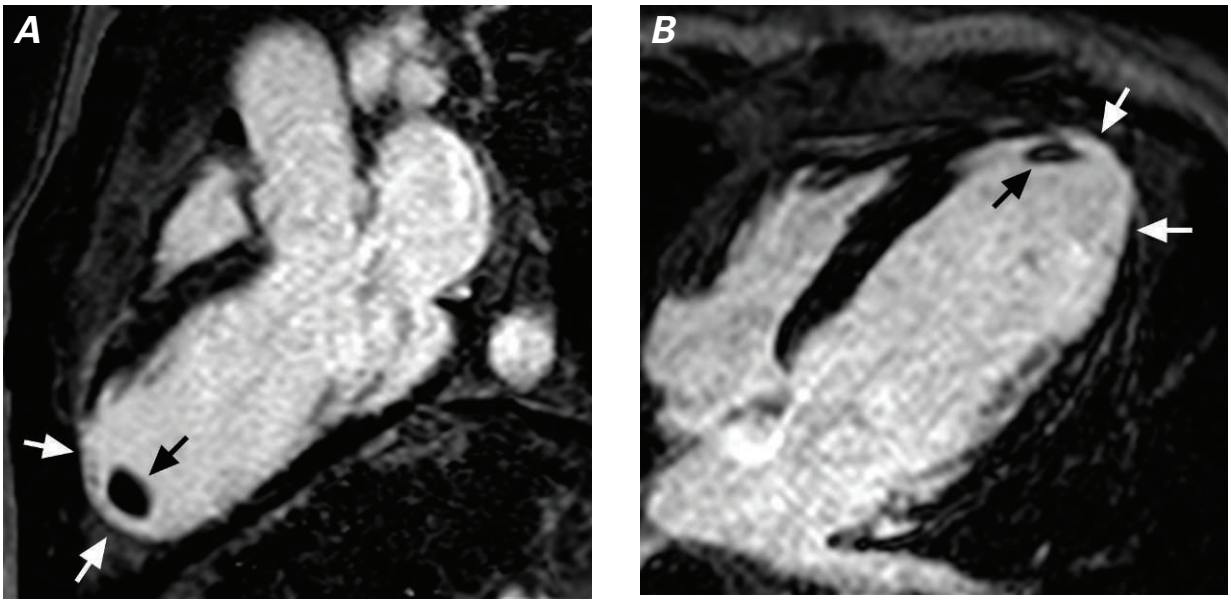

Fig. 2 *Long-axis phase-sensitive inversion-recovery images (**A,** 3-chamber view, and **B**, 4-chamber view) in a patient with coronary artery disease reveal an ischemic pattern of late gadolinium enhancement (brighter myocardium) that extends variably from the subendocardium toward the epicardium in the distal anterior and apical segments (left anterior descending coronary artery distribution) (white arrows). Note the nonenhancing (dark) intraventricular mass-like thrombus (black arrows). The subendocardial location and involvement of segments in a coronary artery distribution suggest an ischemic cause.*

MR include SSFP, hybrid echo planar imaging, and fast GRE. A saturation prepulse is used to accentuate T1 weighting and the regional myocardial signal-intensity changes caused by gadolinium. Cardiac and respiratory motion artifacts are minimized through the use of an ECG-triggered, breath-hold acquisition. Usually, 40 to 60 heartbeats are acquired to cover the entire first pass of gadolinium. Stress images are obtained under vasodilation achieved by infusing adenosine (or a similar agent) before and during the gadolinium administration. Resting perfusion images are obtained 15 minutes later, to allow the gadolinium to clear from the blood pool.

Although quantitative and semiquantitative estimation of myocardial blood flow is possible with DCE-MR, visual evaluation is more common in clinical practice. In a normal scan, the first pass of gadolinium into the myocardium results in a rapid, uniform change in myocardial signal intensity from dark to bright gray throughout the myocardium on both the stress and rest images. Areas that have physiologically significant compromise in myocardial blood flow show a relative reduction of signal intensity during the gadolinium first pass, which is called a "perfusion defect."

Visual analysis of DCE-MR is sensitive, but image artifacts can contribute to reduced specificity for coronary artery disease. To improve the specificity and accuracy of rapid visual evaluation for the detection of coronary artery disease, DCE-MR has been combined with DE-MR in a multicomponent interpretation algorithm (Figs. 3 and 4).[14,15] This algorithm offers the advantage of evaluating in a single study 2 independent, albeit related, downstream effects of coronary artery disease: MI (with DE-MR) and ischemia (with DCE-MR). The robustness of DE-MR can help to overcome some of the imaging artifacts that confound the interpretation of DCE-MR. The presence of an LGE ischemic pattern on DE-MR or a reversible perfusion defect on DCE-MR (perfusion defect on stress imaging but absent on rest imaging) is consistent with coronary artery disease. In the absence of an LGE ischemic pattern on DE-MR, a reversible defect on DCE-MR suggests coronary artery disease without infarction. When both DE-MR and DCE-MR are negative, or when DE-MR is negative and there is a matched defect on DCE-MR (indicating an artifact), the diagnosis of coronary artery disease is excluded.

Delayed contrast-enhancement MR is a promising and evolving tool that is increasingly used in daily practice to detect and evaluate the severity and significance of coronary artery disease. When DCE-MR is used with MPI, the results compare favorably to those of invasive angiography, positron emission tomography (PET), and SPECT.[16,17] Delayed contrast-enhancement MR has also been used to identify microvascular disease in patients with cardiac syndrome X.[18] Signal-intensity changes on DCE-MR correlate with fractional flow reserve on invasive coronary angiography.[19] When compared with radionuclide imaging, MPI with DCE-MR has higher spatial resolution and the ability to identify regional flow differences over the full range of coronary vasodilation without the need for ionizing radiation. When combined with cine MR to detect wall-motion abnormalities and with DE-MR to detect myocardial scar tissue, DCE-MR offers an efficient, comprehensive technique to assist in clinical decision-making and in predicting patient outcomes. However, it should be noted that the use of MPI with CMR is more challenging and less well validated in patients with extensively remodeled LVs and thinned-out myocardium.[20]

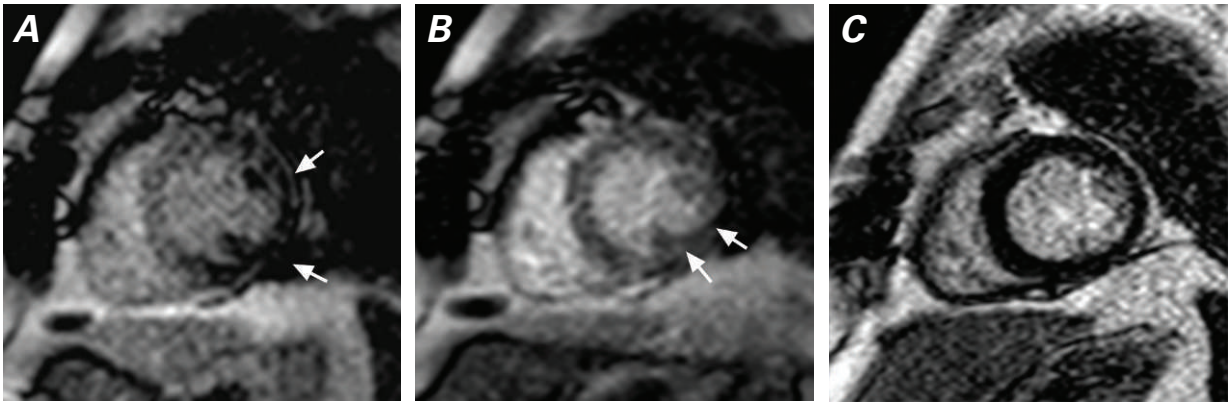

Fig. 3 *Inducible defect.* ***A****) Stress perfusion image obtained during intravenous infusion of adenosine.* ***B****) Resting-state perfusion image. The darkened myocardium in the stress perfusion image in the anterolateral and inferolateral segments (arrows in* ***A****) is not present on the resting-state perfusion image (arrows in* ***B****), thereby indicating an inducible perfusion defect.* ***C****) Phase-sensitive inversion recovery image shows absence of late gadolinium enhancement in the involved segments, indicating severe myocardial ischemia without infarction in the distribution of the left circumflex coronary artery. Invasive coronary angiography confirmed high-grade stenoses in obtuse marginal branches of the left circumflex coronary artery.*

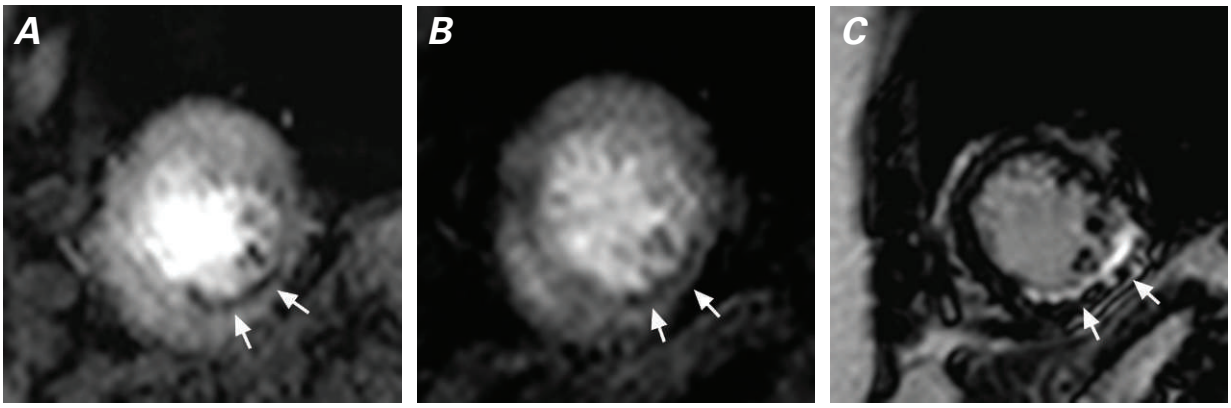

Fig. 4 *Fixed defect.* ***A****) Stress perfusion image obtained during intravenous infusion of adenosine.* ***B****) Resting-state perfusion image. The subtle dark line in the stress perfusion image in the inferolateral and inferior segments (arrows in* ***A****) is also present on the resting-state perfusion image (arrows in* ***B****), thereby indicating a fixed perfusion defect.* ***C****) Phase-sensitive inversion recovery image shows late gadolinium enhancement in an ischemic pattern in these same segments. These findings indicate myocardial infarction without peri-infarct ischemia in the involved segments.*

Evaluation of Nonischemic Cardiomyopathy

Cardiac magnetic resonance imaging has become the preferred technique for characterizing the cause of nonischemic cardiomyopathy, for following disease progression, and for evaluating concomitant pathologic conditions, treatment response, and functional impact on myocardial and valvular function. For the most effective use of these techniques, CMR protocols should be tailored toward the specific clinical question. The application of CMR in a spectrum of phenotypes of nonischemic cardiomyopathies is described below.

Sarcoidosis. Cardiac sarcoidosis has multiple manifestations on CMR. Acute myocardial sarcoidosis can display focal hyperintensity on T2-weighted (T2W) images as a result of myocardial edema and early gadolinium enhancement inflammation. These findings are typically observed in a noncoronary distribution and might be seen even in asymptomatic patients with cardiac sarcoidosis. Focal thickening due to myocardial edema can mimic hypertrophic cardiomyopathy or a cardiac mass.[21] In nodular sarcoidosis, CMR can display central low signal intensity on both T1W and T2W images (representing hyaline fibrotic tissue) and a peripheral area with high signal intensity on T2W images (representing edema).[21]

Cardiac magnetic resonance imaging also enables simultaneous evaluation of regional and global ventricular function and imaging of extracardiac manifestations of sarcoidosis such as intrathoracic adenopathy. Recently, DE-MR has shown promising results for early noninvasive diagnosis of cardiac sarcoidosis. Epicardial or midmyocardial LGE in the anteroseptal and inferolateral segments is considered characteristic of sarcoidosis.[22] However, any territory can be involved (Fig. 5), and the pattern of LGE described for sarcoidosis can be similar to that seen in myocarditis. Rarely, an ischemic pattern of LGE can also be observed in patients with sarcoidosis.[23] Notwithstanding these pitfalls, CMR findings can be used to guide clinicians to a site for endomyocardial biopsy in patients with suspected sarcoidosis. Late gadolinium enhancement on DE-MR is also an independent predictor of adverse clinical events, including cardiac death in patients with cardiac sarcoidosis.[23]

Cardiac magnetic resonance has also been used for follow-up in patients on steroid therapy.[22,24] Late gadolinium enhancement tends to regress early after steroid therapy (<6 mo), whereas regression of edema on T2W images is delayed (>6 mo). These abnormalities tend to persist or increase in severity and extent in nonresponders.[24] However, use of CMR to evaluate the response to treatment will not always be feasible, because some patients with cardiac sarcoidosis end up receiving a defibrillator, which is a contraindication for MR imaging.

Hypertrophic Cardiomyopathy. Cardiac magnetic resonance imaging is being increasingly used to define the phenotypic variability, ventricular function, and hemodynamic states of hypertrophic cardiomyopathy. Cine MR is superior to echocardiography for the identification and quantification of the degree, extent, and distribution of myocardial hypertrophy, particularly in patients with the apical variant of hypertrophic cardiomyopathy.[25,26] Steady-state free precession cine images enable direct visualization of the systolic anterior motion of mitral valve leaflets, mitral regurgitation, and abnormalities of the subvalvular apparatus and papillary muscles. Cine MR imaging can also differentiate obstructive forms of septal hypertrophic cardiomyopathy from nonobstructive forms[27]; obstruction due to hypertrophied myocardium is identified by consequent flow acceleration, turbulence, and signal void on cine MR sequences. Phase-contrast MR is also helpful in showing flow acceleration across the LV outflow tract and in estimating pressure gradient at rest.

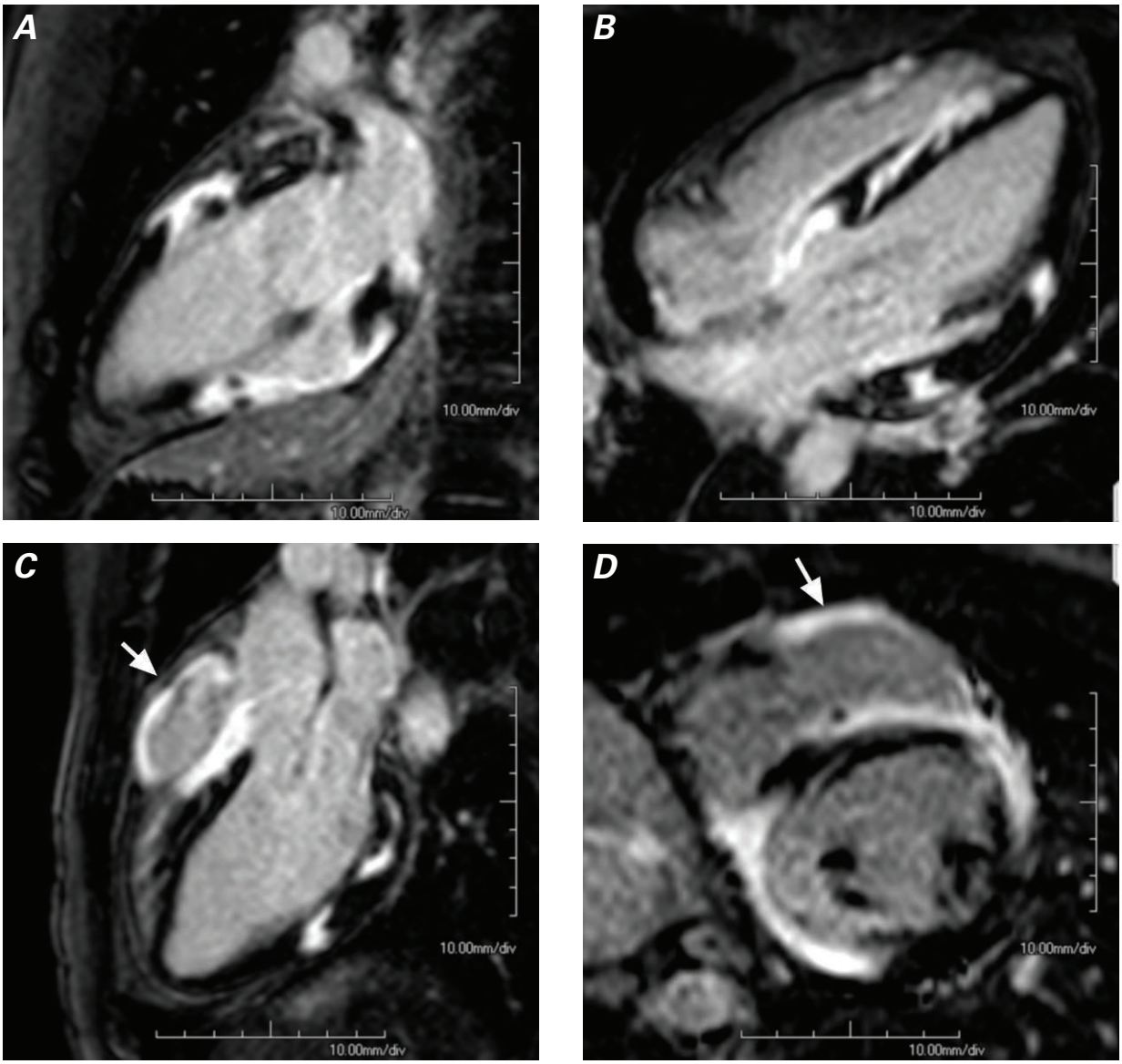

Fig. 5 A–D*) Long-axis and short-axis phase-sensitive inversion recovery images in a patient with biopsy-proven sarcoidosis show myocardial late gadolinium enhancement (LGE) (brighter myocardium) involving the basal and mid left ventricle in a noncoronary distribution. Also note (**C** and **D**) the LGE in the right ventricular wall (arrows). Epicardial or mid-myocardial LGE in the anteroseptal and inferolateral segments is considered characteristic of sarcoidosis.*

Delayed-enhancement MR imaging is used in patients with hypertrophic cardiomyopathy to reveal areas of fibrosis.[28] Late gadolinium enhancement in patients with hypertrophic cardiomyopathy is typically patchy and mid-myocardial; specifically, late gadolinium enhancement tends to affect the hypertrophied segments, the RV free-wall insertion points into the interventricular septum, and the apical segments (in patients with apical variant).[29,30] However, LGE might also be seen in nonhypertrophied segments (Figs. 6 and 7).[31] Late gadolinium enhancement tends to be more prevalent and pronounced in patients with advanced structural disease. The presumed underlying pathophysiologic mechanisms for LGE in patients with hypertrophic cardiomyopathy include increased collagen deposition and micro-ischemia due to abnormal intramural arteries.[28,32] The prognostic significance of LGE in patients with hypertrophic cardiomyopathy is still evolving; however, the extent of LGE is inversely correlated with LV ejection fraction, positively correlated with regional hypertrophy, and linked to the risk of sudden death and development of LV dilation and heart failure.[33,34] Late gadolinium enhancement has also been associated with ventricular arrhythmia on Holter monitoring.[35] Nonetheless, LGE has not yet been established as a criterion for the placement of an implantable defibrillator in patients with hypertrophic cardiomyopathy.[20] Cardiac magnetic resonance imaging with DE-MR is

an ideal technique for screening the immediate relatives of probands because of its phenotypic accuracy and its ability to identify abnormal myocardial substrate linked to adverse events.[4]

Idiopathic Dilated Cardiomyopathy. Cine CMR accurately quantifies global ventricular function and reveals patterns of contractile dysfunction in cases of idiopathic dilated cardiomyopathy. Patients with idiopathic dilated cardiomyopathy manifest global ventricular enlargement and hypokinesis. Although regional variations can be present, segmental wall-motion abnormalities do not necessarily follow coronary artery distributions. On DE-MR, patients with idiopathic dilated cardiomyopathy usually do not exhibit LGE; this lack of LGE can be used as confirmatory evidence for the diagnosis of idiopathic dilated cardiomyopathy in patients with LV dysfunction and might therefore obviate the need for coronary angiography.[4,36] However, in 10% to 28% of patients, a characteristic pattern of mid-myocardial LGE involving the basal or mid-interventricular septum can be seen.[36,37] The pathophysiologic basis of LGE (a nonischemic pattern) in idiopathic dilated cardiomyop-

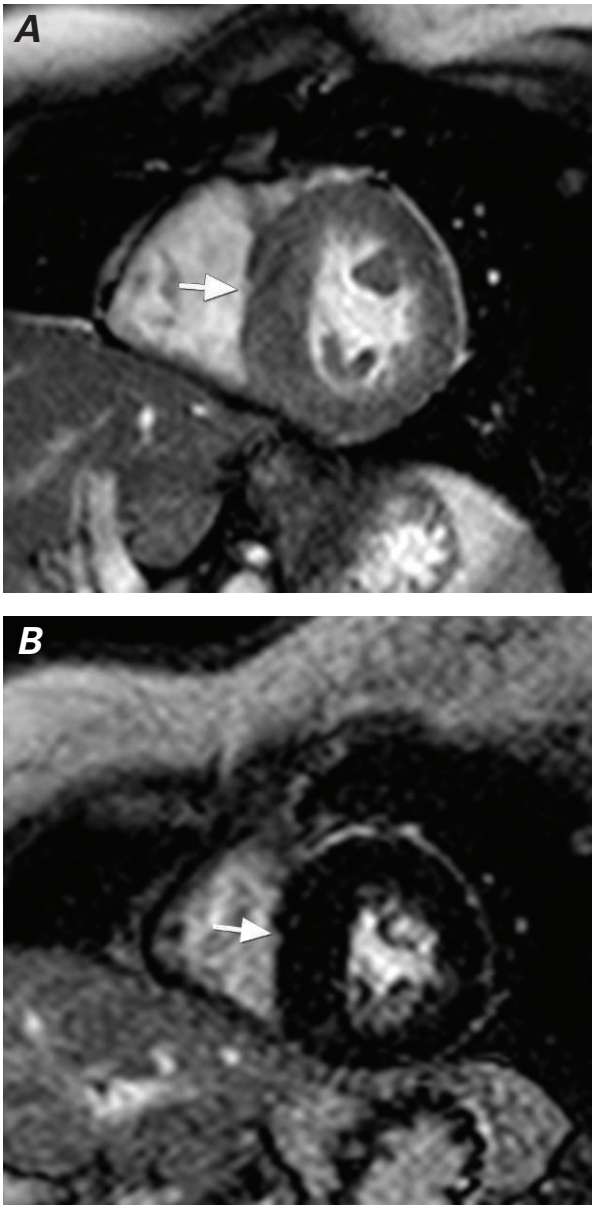

Fig. 6 ***A****) Short-axis cine steady-state free precession image shows moderate hypertrophy of the mid septum in a patient with hypertrophic cardiomyopathy (arrow).* ***B****) Phase-sensitive inversion recovery image shows absence of late gadolinium enhancement in the hypertrophied septum (arrow).*

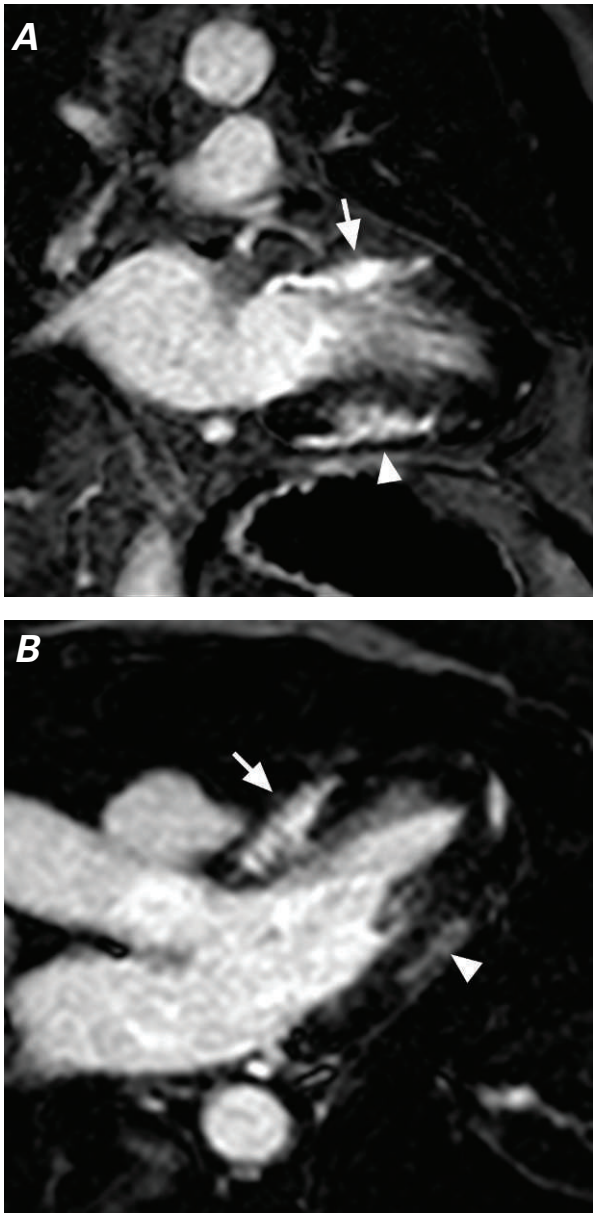

Fig. 7 ***A****) Vertical long-axis and* ***B****) left ventricular outflow tract phase-sensitive inversion recovery images in a patient with hypertrophic cardiomyopathy show marked late gadolinium enhancement in the hypertrophied septum (arrows) and in the lateral and inferior walls (arrowheads).*

athy is not clear. Late gadolinium enhancement might represent either focal segmental fibrosis or a recurrence of previous subclinical myocarditis.[12] Moreover, an ischemic pattern of LGE can occasionally be seen in patients who have been diagnosed with idiopathic dilated cardiomyopathy on the basis of coronary angiographic findings.[36] The ischemic LGE pattern in these patients is presumed to represent coronary artery embolism from minimally stenotic but unstable plaques, vasospasm, or recanalization after an occlusive coronary event.[38] Alternatively, patients with discrepant findings (for example, limited-ischemic-pattern LGE but significant LV dysfunction and dilation) might have both dilated cardiomyopathy and "bystander" coronary artery disease. In such cases, DE-MR can be used to identify underlying coronary artery disease in patients with presumed idiopathic dilated cardiomyopathy.

The extent of LGE has significant prognostic value for patients with idiopathic dilated cardiomyopathy. Late gadolinium enhancement correlates with the severity of LV dysfunction[39] and confers a low likelihood of functional recovery after optimal medical therapy.[40] Late gadolinium enhancement also identifies a subgroup of patients with a higher risk of inducible ventricular arrhythmias on electrophysiologic studies[41] and is an independent predictor of the risk of future cardiovascular events.[42] Cardiac magnetic resonance has also been used for serial evaluation of cardiac function in response to pharmacologic interventions in patients with idiopathic dilated cardiomyopathy.[43]

Amyloidosis. Cardiac magnetic resonance imaging plays a significant role in the evaluation of patients with amyloidosis, who commonly present with a suspected restrictive cardiomyopathy. In patients with amyloidosis, CMR findings include variable degrees of functional impairment, concentric thickening of the ventricular walls, and associated thickening of the interatrial septum and atrial walls. Patients with amyloid restrictive cardiomyopathy can have a characteristic diffuse LGE pattern (Fig. 8), which is usually more prominent in the subendocardium and in the basal segments.[44,45] The pathophysiologic basis of this pattern is presumed to be myocardial interstitium expanded by amyloid deposition and variable degrees of myocardial fibrosis.[38] Late gadolinium enhancement is also a strong independent predictor of 1-year death in patients with cardiac amyloidosis.[46]

Arrhythmogenic Right Ventricular Cardiomyopathy. Cardiac magnetic resonance imaging is the first-line technique for following changes in RV volumes, structure, and function over time and for evaluating suspected RV cardiomyopathy, such as arrhythmogenic RV cardiomyopathy (ARVC). Right ventricular dilation (indexed ED volume, ≥110 mL/m^2 in men or ≥100 mL/m^2 in women), regional wall-motion abnormality, and reduced RV ejection fraction (≤0.40) constitute one of

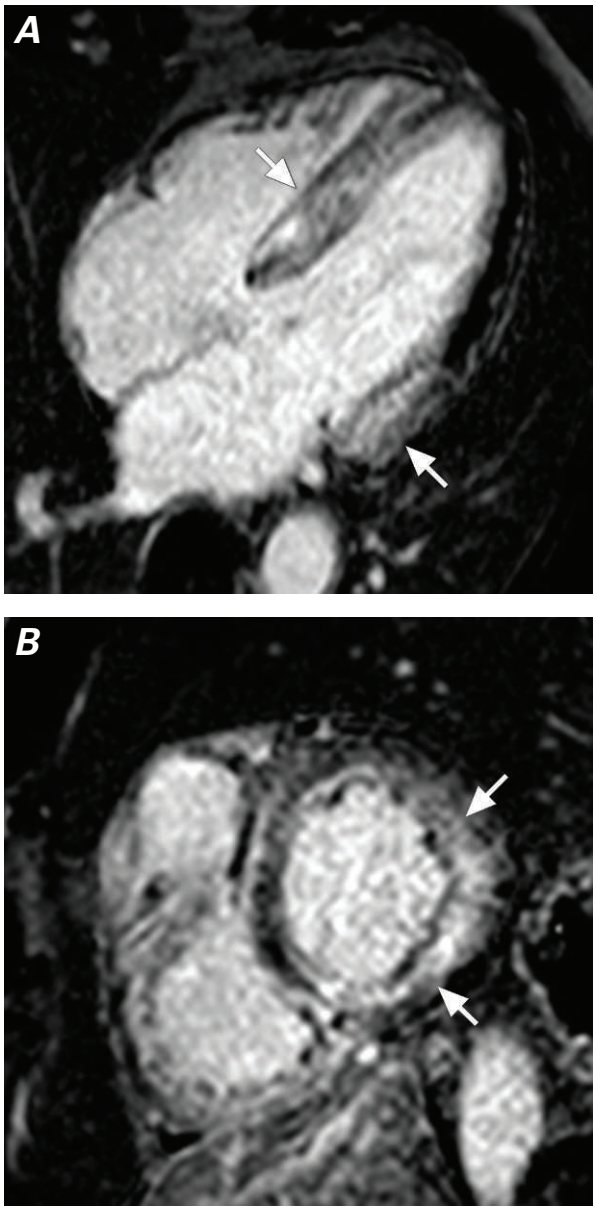

Fig. 8 ***A****) Long-axis and* ***B****) short-axis phase-sensitive inversion recovery images in a patient with biopsy-proven amyloidosis show diffuse late gadolinium enhancement with mild concentric thickening of the left ventricular walls (arrows).*

the major criteria for the diagnosis of ARVC as set forth by the revised Task Force Criteria for the diagnosis of ARVC.[47] Other morphologic RV abnormalities that can be seen in patients with ARVC include thickening (>6 mm) or thinning (<2 mm) of the myocardial wall, focal aneurysms, trabecular disarray, moderator-band hypertrophy, and increased myocardial signal on black-blood images (which suggests fatty infiltration). However, detecting fat in the thin RV free wall and differentiating this fat from adjacent epicardial fat can be challenging and very much dependent upon optimal image quality.[48-50] In patients with proven ARVC, DE-MR per-

formed in concert with fat suppression shows LGE in the RV free wall and in the interventricular septum, which correlates with fibrosis on histopathologic examination. The presence of LGE can predict inducibility of ventricular tachycardia upon electrophysiologic testing. On the basis of these findings, a role for LGE in risk stratification has been proposed.[51] However, LGE is not currently included in the revised Task Force Criteria for the diagnosis of ARVC.

Left Ventricular Noncompaction. Left ventricular noncompaction is morphologically characterized by excessive LV trabeculation; patients with this condition often present with progressive ventricular dysfunction, arrhythmias, or cardioembolism. Recent studies have suggested that CMR is more effective than conventional echocardiography in identifying the extent of noncompaction and providing supplemental morphologic information.[52] Two CMR-based criteria for the diagnosis of LV noncompaction have been proposed: a threshold ratio >2.3 for noncompacted-to-compacted myocardium on diastolic SSFP sequence, long-axis views in patients with a distinct 2-layered appearance of the myocardium[53]; and LV trabecular mass >20% of global LV mass.[54] However, these morphologic diagnostic criteria have not been validated in larger studies.

Delayed-enhancement MR can reveal the characteristic myocardial fibrosis in the deep intertrabecular recesses of the noncompacted myocardium and the related papillary muscles.[53] In patients with LV noncompaction, delayed-enhancement MR is also optimally suited to the display of intertrabecular thrombus, the likely source of cardioembolic phenomena.

Valvular Heart Disease

Cardiac magnetic resonance imaging provides a comprehensive evaluation of valvular stenosis and regurgitation and enables accurate evaluation of the effect of valvular pathologic conditions on cardiac function and anatomy. The role of CMR is often complementary to that of echocardiography and is particularly helpful when findings on echocardiography, clinical examination, and cardiac catheterization are discordant. Anatomic information obtained through CMR about leaflet morphology, thickness, and vegetations might be inferior to information obtained through echocardiography because of CMR's lesser temporal resolution. Cardiac magnetic resonance imaging can also be used to identify abscesses, extracardiac spread of infection, and rupture of the sinus of Valsalva secondary to endocarditis.[55,56]

Jets of flow across regurgitant or stenosed valves lead to signal loss on cine CMR sequences due to intravoxel dephasing of protons as a consequence of the turbulence. Length and area of signal loss are validated as semiquantitative indicators of the severity of valvular pathologic conditions.

For CMR quantification of the severity of valvular pathologic conditions, the technique that is most frequently used in practice is PC-MR. Phase-contrast MR is an accurate, validated, and reproducible technique for measuring flow. Through-plane PC-MR (the velocity jet is perpendicular to the imaging plane) is necessary for flow quantification. Quantification of the RV and LV outputs can also be compared with the use of through-plane flow measurements from the proximal ascending aorta and the pulmonary trunk. In patients with a single regurgitant atrioventricular valve, regurgitant volume quantification can be calculated as the difference between RV and LV stroke volumes.

Valvular Regurgitation. Cardiac magnetic resonance imaging offers accurate definition of the valvular regurgitant jet and quantification of regurgitant volume (both the absolute value and the regurgitant fraction). When combined with information about the functional impact of regurgitation on cardiac volumes and function, data from CMR can guide the timing of valve replacement.

Direct quantification of the regurgitant volume and the regurgitant fraction is performed by measuring the forward systolic and reverse diastolic flow in the ascending aorta by means of PC-MR (Fig. 9). This approach is more accurate than echocardiography, has high reproducibility, and has been used to identify patients with aortic regurgitation who will be responsive to therapy with an angiotensin-converting enzyme inhibitor and hydralazine.[4,57,58] In patients with mitral regurgitation, the jet direction and origin can be optimally portrayed on cine CMR, which can help to discern the mechanism of regurgitation. Cardiac magnetic resonance can also reveal associated structural alterations, including myxomatous, infective, or congenital (cleft, for example) degeneration; annular dilation; papillary muscle rupture; and functional alterations such as prolapsed or flail valve. For regurgitant volume quantification, the forward stroke volume in the ascending aorta as measured by PC-MR is subtracted from the LV stroke volume (obtained from the cine SSFP short-axis LV stack). Direct quantification of mitral regurgitation by performing PC-MR at the level of the mitral inflow is complicated by the through-plane motion of the annulus and the eccentricity of the mitral regurgitation jet,[59] so this technique is less often used.

Valvular Stenosis. Valvular stenosis is identified by signal loss caused by a jet of turbulence distal to an abnormal valve on cine CMR during the appropriate phase of the cardiac cycle. Phase-contrast MR imaging enables quantification of the stenosis severity. Initially, the jet is defined by means of in-plane cine CMR. Quantification is then performed with either through-plane or in-plane imaging at the site of maximum velocity. The Bernoulli equation is used to estimate the pressure gradient. For estimation of the valve area in patients with aortic stenosis, PC-MR is used to calculate the

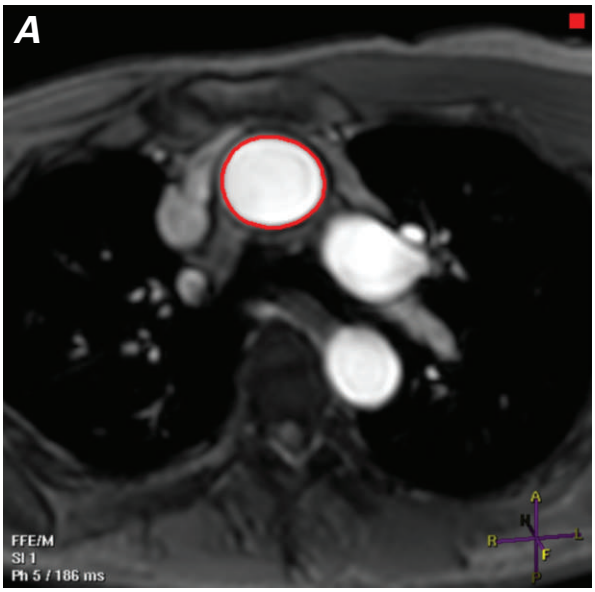

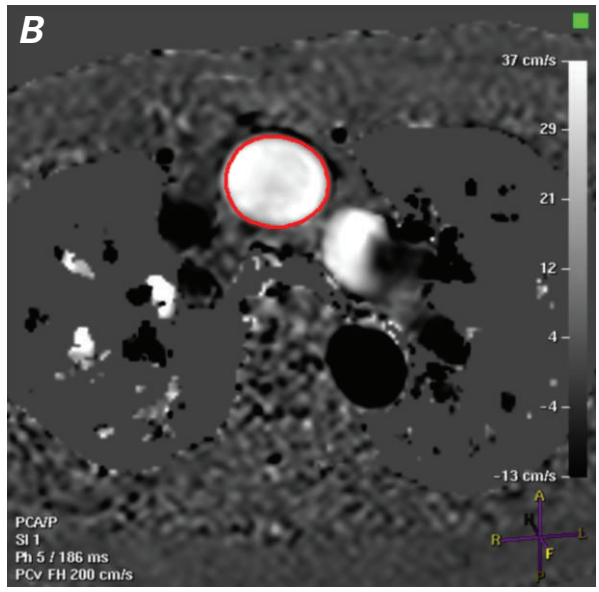

C

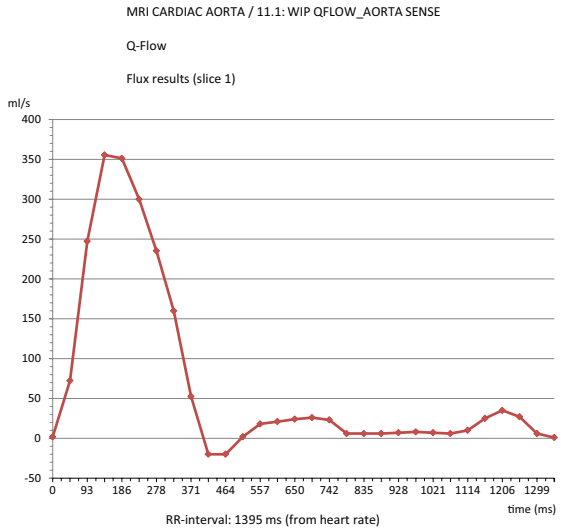

D

ANALYSIS SETTINGS INFORMATION:

Heart rate	:	43 bpm
RR-interval	:	1395 ms (from heart rate)
Cardiac triggering	:	retrospective
Measurement interval	:	1395 ms (RR-interval)

ANALYSIS RESULTS:

slice 1	Vessel 1
Stroke volume (ml)	92.6
Forward flow vol. (ml)	94.1
Backward flow vol. (ml)	1.4
Regurgitant fract. (%)	1.5
Abs. stroke volume (ml)	95.5
Mean flux (ml/s)	66.4
Stroke distance (cm)	8.6
Mean velocity (cm/s)	6.2

Vessel 1, slice 1

Nr	Td ms	Flux ml/s	Area cm2	Area pixels	Mean vel. cm/s	Max. vel. cm/s	Min. vel. cm/s	Peak vel. cm/s	Vel stddev cm/s
1	0	1.8	9.8	624	0.2	6.3	-8.3	-8.3	3.4
2	46	72.3	10.0	640	7.2	19.7	-1.6	19.7	4.6
3	93	247.2	10.3	656	24.1	41.0	12.8	41.0	5.9
4	139	355.5	10.7	684	33.3	48.7	17.6	48.7	6.0
5	186	351.3	10.9	699	32.2	43.6	6.7	43.6	6.0
6	232	299.9	10.9	700	27.4	67.2	-14.9	67.2	15.9
7	278	235.1	10.9	700	21.5	81.2	-29.2	81.2	25.6
8	325	159.8	11.1	713	14.3	68.2	-39.1	68.2	26.9
9	371	52.6	11.2	719	4.7	42.8	-36.8	42.8	22.1

Fig. 9 *Through-plane quantitative flow images through the ascending aorta.* ***A****) Magnitude image details the anatomy, contour, and shape of the vessel, whereas* ***B****) the phase-velocity map displays the direction of flow.* ***C****) Region of interest is contoured over the ascending aorta to measure the flow throughout the cardiac cycle.* ***D****) The software generates the settings information and detailed analysis results for each frame.*

velocity profiles in the LV outflow tract and in the ascending aorta. The continuity equation is then applied to calculate the valve area. The mitral valve area can also be estimated from the PC-MR–derived mitral pressure half-time. Reversal of the pulmonary vein flow detected by PC-MR is a sign of severe mitral stenosis. Finally, CMR also enables concomitant evaluation of the consequences of mitral stenosis, such as left atrial enlargement, atrial thrombi in patients with atrial fibrillation, and pulmonary hypertension and its secondary effects, such as RV dysfunction and pulmonary regurgitation.

Cardiac magnetic resonance-derived values correlate with results from catheterization and Doppler echocardiography in patients with mitral and aortic valve stenosis.[60,61] Cardiac magnetic resonance has an advantage over echocardiography, because the velocity jet can be aligned easily in any direction in CMR, without the limitation of acoustic windows. Cardiac magnetic resonance can also be used to evaluate pulmonary and tricuspid valve pathologic conditions and their effects on cardiac volumes and function, and it is particularly valuable in patients who have multivalve disease.

Pericardial Disease

Cardiac magnetic resonance imaging has become the gold-standard noninvasive technique for the evaluation of pericardial disease. This technique is able to evaluate pericardial morphology and its functional impact on diastolic cardiac function and heart filling. Free-breathing, real-time cine CMR is a key sequence for the evaluation of pericardial pathologic conditions, because this technique directly shows the effect of the pericardium on dynamic, physiologic events, thereby identifying the respirophasic variation of the interventricular septum during free breathing.[62]

Congenital Pericardial Pathologic Conditions. Pericardial cysts are well-circumscribed, simple-appearing cysts, typically in the cardiophrenic angles that are attached to the pericardium either directly or through a peduncle. In contrast, a pericardial diverticulum appears as a focal outpouching that maintains a direct communication with the pericardial sac. The diagnosis of congenital pericardial defect on CMR has its basis in indirect findings associated with the absence of an intact pericardium. These include abnormal cardiac position (such as excessive levorotation), abnormal indentation of a cardiac chamber at the location of the defect, and herniation of the lung tissue through the defect.

Acquired Pericardial Pathologic Conditions. The presence of pericardial LGE on DE-MR with or without small effusion supports a clinical diagnosis of acute pericarditis.[63] The high spatial resolution of DE-MR enables the evaluation of adjacent epicardial fat and myocardial involvement in the inflammatory process. Cardiac magnetic resonance imaging is also complementary to, and can be more advantageous than, echocardiography for the evaluation of pericardial effusion. In particular, CMR is more effective than echocardiography in detecting and characterizing small, loculated, or nonserous effusions (Fig. 10). Moreover, CMR can provide clues to the presence of unsuspected pericardial tamponade. Findings that suggest tamponade include diastolic wall-flattening or inversion of the right-sided chambers, early diastolic paradoxical bouncing of the interventricular septum ("septal bounce"), and flattening or inversion of the septum on deep-breathing real-time cine imaging. These findings indicate reduced ventricular compliance; augmentation of RV filling during normal breathing and on deep inspiration occurs at the expense of diminished LV filling.

The most important indication, however, is constrictive pericarditis, or the suspicion of it. Morphologic findings for constrictive pericarditis include focal or generalized pericardial thickening with irregular margins and a tubular configuration of the ventricles due to the effect of a noncompliant pericardium. Ancillary findings include atrial dilation, pleural effusion, venous distention, and (in the included upper abdominal images) hepatomegaly and ascites. Although significant pericardial thickening (>5–6 mm) is traditionally considered an important diagnostic criterion for constrictive pericarditis, recent studies have challenged this notion[64]—there appears to be only a weak correlation between the extent of pericardial thickening and the severity of constrictive pericarditis.[65] In fact, end-stage irreversible constrictive pericarditis can be associated with a thin pericardium.[66,67]

Pericardial LGE in patients with constrictive pericarditis suggests residual pericardial inflammation (Fig. 11) and correlates with organizing pericarditis on histopathologic examination.[66] When seen in conjunction with inflammatory biomarkers, pericardial LGE is a potential predictor of the reversibility of constrictive

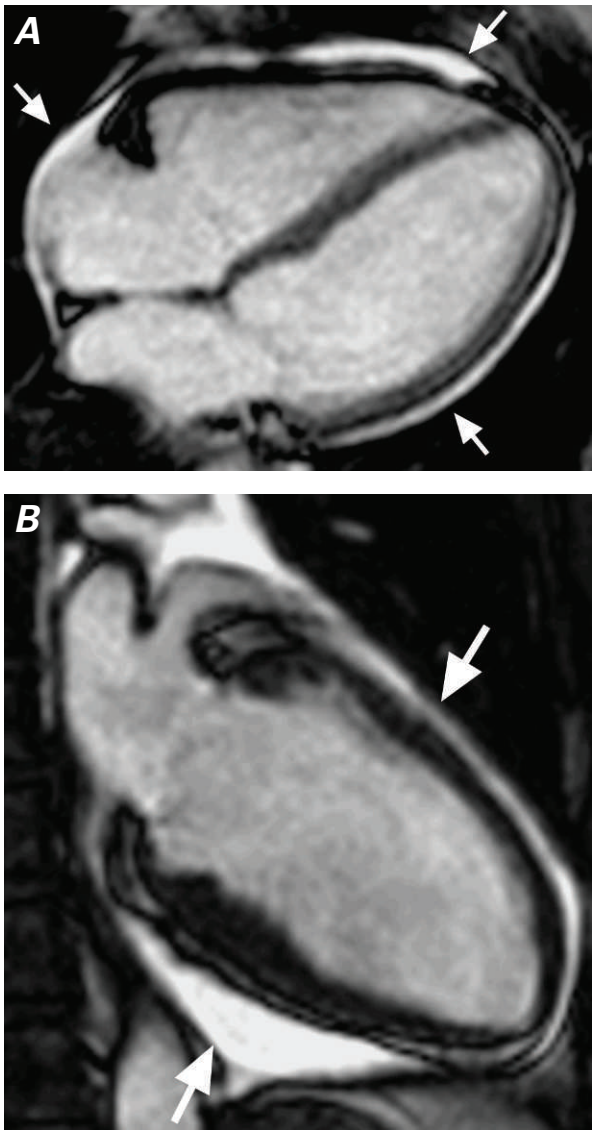

Fig. 10 ***A****) and* ***B****) Long-axis cine steady-state free precession images show a circumferential simple pericardial effusion, which appears as bright, fluid-signal intensity in the pericardial sac (arrows).*

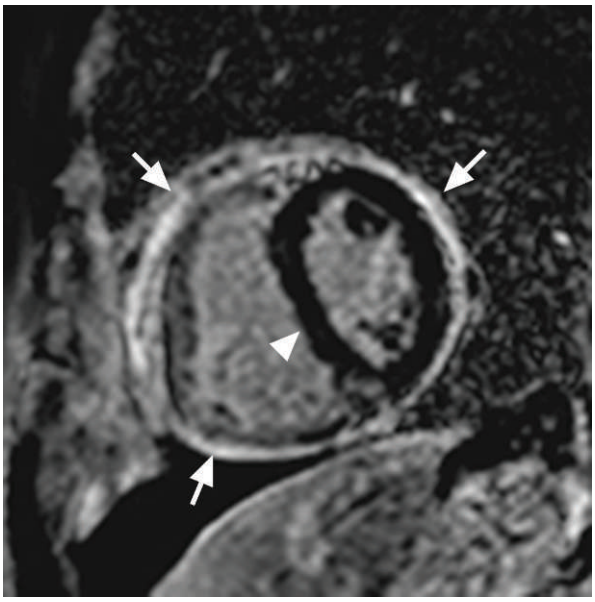

Fig. 11 *Short-axis phase-sensitive inversion recovery image in a patient with constrictive pericarditis shows moderate circumferential pericardial late gadolinium enhancement (arrows), indicating pericardial inflammation. Note the flattened interventricular septum (arrowhead), consistent with equalization of ventricular pressures.*

pericarditis with medical management alone. The diagnosis of constrictive pericarditis is particularly challenging, because it involves close study of both functional and hemodynamic alterations to identify "constrictive physiology." Findings of constrictive physiology include diastolic septal bounce on cine MR and early inspiratory septal flattening or inversion on real-time cine CMR. Diastolic septal bounce has a high sensitivity and specificity for the diagnosis of constrictive pericarditis.[68] Evidence of interventricular septal respirophasic variation on CMR is also considered a hallmark of constrictive pericarditis; this finding is not seen in restrictive cardiomyopathy.[69] Phase-contrast MR can be used to discern a restrictive filling pattern across the tricuspid valve and in the inferior vena cava in patients with constrictive pericarditis.[70] Fibrotic adhesion between the pericardial layers and the extension of the fibrotic process into the adjacent myocardium can be recognized on MR tagging by the persistence of grid lines throughout the cardiac cycle.[71]

Please see the next issue for Part 2 of this article, which will focus on emerging applications of CMR imaging for the investigation of cardiovascular disorders.

Acknowledgment

We are grateful for the editorial assistance of Megan M. Griffiths, scientific writer for the Imaging Institute, Cleveland Clinic.

References

1. Grothues F, Smith GC, Moon JC, Bellenger NG, Collins P, Klein HU, Pennell DJ. Comparison of interstudy reproducibility of cardiovascular magnetic resonance with two-dimensional echocardiography in normal subjects and in patients with heart failure or left ventricular hypertrophy. Am J Cardiol 2002;90(1):29-34.
2. Bottini PB, Carr AA, Prisant LM, Flickinger FW, Allison JD, Gottdiener JS. Magnetic resonance imaging compared to echocardiography to assess left ventricular mass in the hypertensive patient. Am J Hypertens 1995;8(3):221-8.
3. Bellenger NG, Davies LC, Francis JM, Coats AJ, Pennell DJ. Reduction in sample size for studies of remodeling in heart failure by the use of cardiovascular magnetic resonance. J Cardiovasc Magn Reson 2000;2(4):271-8.
4. Pennell DJ, Sechtem UP, Higgins CB, Manning WJ, Pohost GM, Rademakers FE, et al. Clinical indications for cardiovascular magnetic resonance (CMR): Consensus Panel report. Eur Heart J 2004;25(21):1940-65.
5. Caudron J, Fares J, Bauer F, Dacher JN. Evaluation of left ventricular diastolic function with cardiac MR imaging. Radiographics 2011;31(1):239-59.
6. Pineda V, Merino X, Gispert S, Mahia P, Garcia B, Dominguez-Oronoz R. No-reflow phenomenon in cardiac MRI: diagnosis and clinical implications. AJR Am J Roentgenol 2008;191(1):73-9.
7. Choi KM, Kim RJ, Gubernikoff G, Vargas JD, Parker M, Judd RM. Transmural extent of acute myocardial infarction predicts long-term improvement in contractile function. Circulation 2001;104(10):1101-7.
8. Kim RJ, Wu E, Rafael A, Chen EL, Parker MA, Simonetti O, et al. The use of contrast-enhanced magnetic resonance imaging to identify reversible myocardial dysfunction. N Engl J Med 2000;343(20):1445-53.
9. Selvanayagam JB, Kardos A, Francis JM, Wiesmann F, Petersen SE, Taggart DP, Neubauer S. Value of delayed-enhancement cardiovascular magnetic resonance imaging in predicting myocardial viability after surgical revascularization. Circulation 2004;110(12):1535-41.
10. Wagner A, Mahrholdt H, Holly TA, Elliott MD, Regenfus M, Parker M, et al. Contrast-enhanced MRI and routine single photon emission computed tomography (SPECT) perfusion imaging for detection of subendocardial myocardial infarcts: an imaging study. Lancet 2003;361(9355):374-9.
11. Kim RJ, Fieno DS, Parrish TB, Harris K, Chen EL, Simonetti O, et al. Relationship of MRI delayed contrast enhancement to irreversible injury, infarct age, and contractile function. Circulation 1999;100(19):1992-2002.
12. Mahrholdt H, Goedecke C, Wagner A, Meinhardt G, Athanasiadis A, Vogelsberg H, et al. Cardiovascular magnetic resonance assessment of human myocarditis: a comparison to histology and molecular pathology. Circulation 2004;109(10):1250-8.
13. Goenka AH, Das CJ, Sharma R. Nephrogenic systemic fibrosis: a review of the new conundrum. Natl Med J India 2009;22(6):302-6.
14. Cury RC, Cattani CA, Gabure LA, Racy DJ, de Gois JM, Siebert U, et al. Diagnostic performance of stress perfusion and delayed-enhancement MR imaging in patients with coronary artery disease. Radiology 2006;240(1):39-45.
15. Klem I, Heitner JF, Shah DJ, Sketch MH Jr, Behar V, Weinsaft J, et al. Improved detection of coronary artery disease by stress perfusion cardiovascular magnetic resonance with the use of delayed enhancement infarction imaging. J Am Coll Cardiol 2006;47(8):1630-8.

16. Panting JR, Gatehouse PD, Yang GZ, Jerosch-Herold M, Wilke N, Firmin DN, Pennell DJ. Echo-planar magnetic resonance myocardial perfusion imaging: parametric map analysis and comparison with thallium SPECT. J Magn Reson Imaging 2001;13(2):192-200.
17. Schwitter J, Nanz D, Kneifel S, Bertschinger K, Buchi M, Knusel PR, et al. Assessment of myocardial perfusion in coronary artery disease by magnetic resonance: a comparison with positron emission tomography and coronary angiography. Circulation 2001;103(18):2230-5.
18. Panting JR, Gatehouse PD, Yang GZ, Grothues F, Firmin DN, Collins P, Pennell DJ. Abnormal subendocardial perfusion in cardiac syndrome X detected by cardiovascular magnetic resonance imaging. N Engl J Med 2002;346(25):1948-53.
19. Rieber J, Huber A, Erhard I, Mueller S, Schweyer M, Koenig A, et al. Cardiac magnetic resonance perfusion imaging for the functional assessment of coronary artery disease: a comparison with coronary angiography and fractional flow reserve. Eur Heart J 2006;27(12):1465-71.
20. To AC, Desai MY. Role of cardiac magnetic resonance imaging in assessing ischemic and nonischemic cardiomyopathies. Expert Rev Cardiovasc Ther 2012;10(2):223-33.
21. Vignaux O. Cardiac sarcoidosis: spectrum of MRI features. AJR Am J Roentgenol 2005;184(1):249-54.
22. Shimada T, Shimada K, Sakane T, Ochiai K, Tsukihashi H, Fukui M, et al. Diagnosis of cardiac sarcoidosis and evaluation of the effects of steroid therapy by gadolinium-DTPA-enhanced magnetic resonance imaging. Am J Med 2001;110 (7):520-7.
23. Patel MR, Cawley PJ, Heitner JF, Klem I, Parker MA, Jaroudi WA, et al. Detection of myocardial damage in patients with sarcoidosis. Circulation 2009;120(20):1969-77.
24. Vignaux O, Dhote R, Duboc D, Blanche P, Dusser D, Weber S, Legmann P. Clinical significance of myocardial magnetic resonance abnormalities in patients with sarcoidosis: a 1-year follow-up study. Chest 2002;122(6):1895-901.
25. Rickers C, Wilke NM, Jerosch-Herold M, Casey SA, Panse P, Panse N, et al. Utility of cardiac magnetic resonance imaging in the diagnosis of hypertrophic cardiomyopathy. Circulation 2005;112(6):855-61.
26. Sardanelli F, Molinari G, Petillo A, Ottonello C, Parodi RC, Masperone MA, et al. MRI in hypertrophic cardiomyopathy: a morphofunctional study. J Comput Assist Tomogr 1993;17 (6):862-72.
27. Park JH, Kim YM, Chung JW, Park YB, Han JK, Han MC. MR imaging of hypertrophic cardiomyopathy. Radiology 1992;185(2):441-6.
28. Moon JC, Reed E, Sheppard MN, Elkington AG, Ho SY, Burke M, et al. The histologic basis of late gadolinium enhancement cardiovascular magnetic resonance in hypertrophic cardiomyopathy. J Am Coll Cardiol 2004;43 (12):2260-4.
29. Choudhury L, Mahrholdt H, Wagner A, Choi KM, Elliott MD, Klocke FJ, et al. Myocardial scarring in asymptomatic or mildly symptomatic patients with hypertrophic cardiomyopathy. J Am Coll Cardiol 2002;40(12):2156-64.
30. Teraoka K, Hirano M, Ookubo H, Sasaki K, Katsuyama H, Amino M, et al. Delayed contrast enhancement of MRI in hypertrophic cardiomyopathy [published erratum appears in Magn Reson Imaging 2004;22(6):901]. Magn Reson Imaging 2004;22(2):155-61.
31. Guo ZY, Chen J, Liang QZ, Liao HY, Fu SX, Tang QY, et al. Delay enhancement patterns in apical hypertrophic cardiomyopathy by phase-sensitive inversion recovery sequence. Asian Pac J Trop Med 2012;5(10):828-30.
32. Maron BJ, Wolfson JK, Epstein SE, Roberts WC. Intramural ("small vessel") coronary artery disease in hypertrophic cardiomyopathy. J Am Coll Cardiol 1986;8(3):545-57.
33. Moon JC, McKenna WJ, McCrohon JA, Elliott PM, Smith GC, Pennell DJ. Toward clinical risk assessment in hypertrophic cardiomyopathy with gadolinium cardiovascular magnetic resonance. J Am Coll Cardiol 2003;41(9):1561-7.
34. O'Hanlon R, Grasso A, Roughton M, Moon JC, Clark S, Wage R, et al. Prognostic significance of myocardial fibrosis in hypertrophic cardiomyopathy. J Am Coll Cardiol 2010;56 (11):867-74.
35. Kwon DH, Setser RM, Popovic ZB, Thamilarasan M, Sola S, Schoenhagen P, et al. Association of myocardial fibrosis, electrocardiography and ventricular tachyarrhythmia in hypertrophic cardiomyopathy: a delayed contrast enhanced MRI study. Int J Cardiovasc Imaging 2008;24(6):617-25.
36. McCrohon JA, Moon JC, Prasad SK, McKenna WJ, Lorenz CH, Coats AJ, Pennell DJ. Differentiation of heart failure related to dilated cardiomyopathy and coronary artery disease using gadolinium-enhanced cardiovascular magnetic resonance. Circulation 2003;108(1):54-9.
37. Soriano CJ, Ridocci F, Estornell J, Jimenez J, Martinez V, De Velasco JA. Noninvasive diagnosis of coronary artery disease in patients with heart failure and systolic dysfunction of uncertain etiology, using late gadolinium-enhanced cardiovascular magnetic resonance. J Am Coll Cardiol 2005; 45(5):743-8.
38. White JA, Patel MR. The role of cardiovascular MRI in heart failure and the cardiomyopathies. Magn Reson Imaging Clin N Am 2007;15(4):541-64, vi.
39. Koito H, Suzuki J, Ohkubo N, Ishiguro Y, Iwasaka T, Inada M. Gadolinium-diethylenetriamine pentaacetic acid enhanced magnetic resonance imaging of dilated cardiomyopathy: clinical significance of abnormally high signal intensity of left ventricular myocardium [in Japanese]. J Cardiol 1996;28 (1):41-9.
40. Park S, Choi BW, Rim SJ, Shim CY, Ko YG, Kang SM, et al. Delayed hyperenhancement magnetic resonance imaging is useful in predicting functional recovery of nonischemic left ventricular systolic dysfunction. J Card Fail 2006;12(2):93-9.
41. Nazarian S, Bluemke DA, Lardo AC, Zviman MM, Watkins SP, Dickfeld TL, et al. Magnetic resonance assessment of the substrate for inducible ventricular tachycardia in nonischemic cardiomyopathy. Circulation 2005;112(18):2821-5.
42. Assomull RG, Prasad SK, Lyne J, Smith G, Burman ED, Khan M, et al. Cardiovascular magnetic resonance, fibrosis, and prognosis in dilated cardiomyopathy. J Am Coll Cardiol 2006;48(10):1977-85.
43. Doherty NE 3rd, Seelos KC, Suzuki J, Caputo GR, O'Sullivan M, Sobol SM, et al. Application of cine nuclear magnetic resonance imaging for sequential evaluation of response to angiotensin-converting enzyme inhibitor therapy in dilated cardiomyopathy. J Am Coll Cardiol 1992;19(6):1294-302.
44. Perugini E, Rapezzi C, Piva T, Leone O, Bacchi-Reggiani L, Riva L, et al. Non-invasive evaluation of the myocardial substrate of cardiac amyloidosis by gadolinium cardiac magnetic resonance. Heart 2006;92(3):343-9.
45. Maceira AM, Joshi J, Prasad SK, Moon JC, Perugini E, Harding I, et al. Cardiovascular magnetic resonance in cardiac amyloidosis. Circulation 2005;111(2):186-93.
46. Austin BA, Tang WH, Rodriguez ER, Tan C, Flamm SD, Taylor DO, et al. Delayed hyper-enhancement magnetic resonance imaging provides incremental diagnostic and prognostic utility in suspected cardiac amyloidosis. JACC Cardiovasc Imaging 2009;2(12):1369-77.
47. Marcus FI, McKenna WJ, Sherrill D, Basso C, Bauce B, Bluemke DA, et al. Diagnosis of arrhythmogenic right ventricular cardiomyopathy/dysplasia: proposed modification of the task force criteria. Circulation 2010;121(13):1533-41.

48. Bomma C, Rutberg J, Tandri H, Nasir K, Roguin A, Tichnell C, et al. Misdiagnosis of arrhythmogenic right ventricular dysplasia/cardiomyopathy. J Cardiovasc Electrophysiol 2004; 15(3):300-6.
49. Burke AP, Farb A, Tashko G, Virmani R. Arrhythmogenic right ventricular cardiomyopathy and fatty replacement of the right ventricular myocardium: are they different diseases? Circulation 1998;97(16):1571-80.
50. Tandri H, Castillo E, Ferrari VA, Nasir K, Dalal D, Bomma C, et al. Magnetic resonance imaging of arrhythmogenic right ventricular dysplasia: sensitivity, specificity, and observer variability of fat detection versus functional analysis of the right ventricle. J Am Coll Cardiol 2006;48(11):2277-84.
51. Tandri H, Saranathan M, Rodriguez ER, Martinez C, Bomma C, Nasir K, et al. Noninvasive detection of myocardial fibrosis in arrhythmogenic right ventricular cardiomyopathy using delayed-enhancement magnetic resonance imaging. J Am Coll Cardiol 2005;45(1):98-103.
52. Thuny F, Jacquier A, Jop B, Giorgi R, Gaubert JY, Bartoli JM, et al. Assessment of left ventricular non-compaction in adults: side-by-side comparison of cardiac magnetic resonance imaging with echocardiography. Arch Cardiovasc Dis 2010; 103(3):150-9.
53. Petersen SE, Selvanayagam JB, Wiesmann F, Robson MD, Francis JM, Anderson RH, et al. Left ventricular non-compaction: insights from cardiovascular magnetic resonance imaging. J Am Coll Cardiol 2005;46(1):101-5.
54. Jacquier A, Thuny F, Jop B, Giorgi R, Cohen F, Gaubert JY, et al. Measurement of trabeculated left ventricular mass using cardiac magnetic resonance imaging in the diagnosis of left ventricular non-compaction. Eur Heart J 2010;31(9):1098-104.
55. Akins EW, Slone RM, Wiechmann BN, Browning M, Martin TD, Mayfield WR. Perivalvular pseudoaneurysm complicating bacterial endocarditis: MR detection in five cases. AJR Am J Roentgenol 1991;156(6):1155-8.
56. Hoey ET, Ganeshan A, Nadar SK, Gulati GS. Evaluation of the aortic root with MRI and MDCT angiography: spectrum of disease findings. AJR Am J Roentgenol 2012;199(2): W175-86.
57. Globits S, Blake L, Bourne M, Fujita N, Duerinckx A, Szolar D, et al. Assessment of hemodynamic effects of angiotensin-converting enzyme inhibitor therapy in chronic aortic regurgitation by using velocity-encoded cine magnetic resonance imaging. Am Heart J 1996;131(2):289-93.
58. Hoffmann U, Frank H, Stefenelli T, Kaiser B, Klaar U, Globits S. Afterload reduction in severe aortic regurgitation. J Magn Reson Imaging 2001;14(6):693-7.
59. Fujita N, Chazouilleres AF, Hartiala JJ, O'Sullivan M, Heidenreich P, Kaplan JD, et al. Quantification of mitral regurgitation by velocity-encoded cine nuclear magnetic resonance imaging. J Am Coll Cardiol 1994;23(4):951-8.
60. Caruthers SD, Lin SJ, Brown P, Watkins MP, Williams TA, Lehr KA, Wickline SA. Practical value of cardiac magnetic resonance imaging for clinical quantification of aortic valve stenosis: comparison with echocardiography. Circulation 2003;108(18):2236-43.
61. Kilner PJ, Manzara CC, Mohiaddin RH, Pennell DJ, Sutton MG, Firmin DN, et al. Magnetic resonance jet velocity mapping in mitral and aortic valve stenosis. Circulation 1993; 87(4):1239-48.
62. Francone M, Dymarkowski S, Kalantzi M, Bogaert J. Real-time cine MRI of ventricular septal motion: a novel approach to assess ventricular coupling. J Magn Reson Imaging 2005; 21(3):305-9.
63. Taylor AM, Dymarkowski S, Verbeken EK, Bogaert J. Detection of pericardial inflammation with late-enhancement cardiac magnetic resonance imaging: initial results. Eur Radiol 2006;16(3):569-74.
64. Talreja DR, Edwards WD, Danielson GK, Schaff HV, Tajik AJ, Tazelaar HD, et al. Constrictive pericarditis in 26 patients with histologically normal pericardial thickness. Circulation 2003;108(15):1852-7.
65. Troughton RW, Asher CR, Klein AL. Pericarditis. Lancet 2004;363(9410):717-27.
66. Zurick AO, Bolen MA, Kwon DH, Tan CD, Popovic ZB, Rajeswaran J, et al. Pericardial delayed hyperenhancement with CMR imaging in patients with constrictive pericarditis undergoing surgical pericardiectomy: a case series with histopathological correlation. JACC Cardiovasc Imaging 2011;4 (11):1180-91.
67. Feng D, Glockner J, Kim K, Martinez M, Syed IS, Araoz P, et al. Cardiac magnetic resonance imaging pericardial late gadolinium enhancement and elevated inflammatory markers can predict the reversibility of constrictive pericarditis after antiinflammatory medical therapy: a pilot study. Circulation 2011;124(17):1830-7.
68. Giorgi B, Mollet NR, Dymarkowski S, Rademakers FE, Bogaert J. Clinically suspected constrictive pericarditis: MR imaging assessment of ventricular septal motion and configuration in patients and healthy subjects. Radiology 2003;228 (2):417-24.
69. Francone M, Dymarkowski S, Kalantzi M, Rademakers FE, Bogaert J. Assessment of ventricular coupling with real-time cine MRI and its value to differentiate constrictive pericarditis from restrictive cardiomyopathy. Eur Radiol 2006;16(4):944-51.
70. Bogaert J, Francone M. Pericardial disease: value of CT and MR imaging. Radiology 2013;267(2):340-56.
71. Kojima S, Yamada N, Goto Y. Diagnosis of constrictive pericarditis by tagged cine magnetic resonance imaging. N Engl J Med 1999;341(5):373-4.